STUDY AND DESIGN OF AN ACTIVE TRUNK EXOSKELETON WITH A NON-CONVENTIONAL STRUCTURE

ISSN 1590-8844
International Journal of Mechanics and Control, Vol. 27, No. 01, 2026
https://doi.org/10.69076/jomac.2026.0000

STUDY AND DESIGN OF AN ACTIVE TRUNK EXOSKELETON WITH A NON-CONVENTIONAL STRUCTURE

Gabriella Eula* Luigi Mazza* Terenziano Raparelli* Alberto Vignolo**

* Department of Mechanical and Aerospace Engineering, Politecnico di Torino, Torino Italy

** Master of Science in Mechanical Engineering, Politecnico di Torino, Torino Italy

ABSTRACT

This article presents an active industrial trunk support exoskeleton design with a non-conventional structure. A earlier design was improved, eliminating the leg links and placing two active multifunctional pneumatic actuation groups at the sides of the wearer's trunk. The backframe along the wearer's back was also eliminated, with an eye to having its function performed via the actuation groups themselves and a textile vest that can be stiffened if necessary with elastic bands inserted into pockets in the fabric. In the future, the authors plan to design an alternative solution using electric actuators. Experimental tests were carried out with a volunteer to gain a better understanding of the physiological trunk movement, while future tests will be conducted with a larger number of individuals and AI pose estimation models. Results proved useful for design optimization. The exoskeleton structure provides excellent wearability, compact dimensions, can be further optimized in weight, and is designed to fit a near-universal range of wearers.

Keywords: active trunk exoskeleton; non-conventional trunk exoskeletons; pneumatically controlled trunk exoskeleton; innovative trunk exoskeleton without leg-link

1 INTRODUCTION

Over the past several years, advances in new technologies and robotics [1-4] have fueled the spread of wearable machines, i.e., exoskeletons. Exoskeletons have been used for a variety of purposes including military, rehabilitation and nursing applications, and, more recently, industry. In the industrial sector, many types of active and passive exoskeletons have been developed [5-8] to support the trunk, arms or lower limbs, and to aid in lifting loads and maintaining a mobile sitting position. Wearable robotic exoskeletons are used in industry to support the wearer in a variety of tasks. They reduce musculoskeletal fatigue, enhance the wearer's performance and make workplace accidents less likely [9-11]. Obviously, wearer safety and comfort is a prime consideration in the use of these devices. Care must be taken to ensure that they do not put excessive stress on the wearer's body, especially in the long term, and that they are always used for their intended purpose. Ongoing studies conducted on volunteers have highlighted these devices' usefulness, and 9 out of 10 workers report that wearing an exoskeleton has improved their working lives [10]. In any case, long-term evaluations will be necessary to assess the effects these devices may have on the body of a worker wearing them, performing certain tasks, and using the device for many hours a day and for several consecutive days. This is particularly important given that the relationship between man and machine has become ever closer over the years, to the point that robots have in some cases been replaced with wearable exoskeletons. Physically demanding sectors such as agriculture, construction, and industrial mechanical production and logistics have received the most attention in this respect, as workers exert considerable effort in repetitive tasks that impose high stresses on the spinal column [12-17]. Currently, other authors have presented trunk support exoskeletons [9-11] with no leg links, though most designs feature leg links as well as a backframe [18]. They are in general wearable robots capable of limiting muscle fatigue in the lumbar region and reducing dangerous compressive loads on the spine. Patents have been filed for exoskeletons supporting

Contact author: Gabriella Eula
[1] Dept. of Mechanical and Aerospace Engineering.
E-mail: gabriella.eula@polito.it

the wearer's trunk while bending forward for many hours, some dating from as early as the beginning of the twentieth century [19] and having important applications in agriculture. Some of these designs are also interesting in terms of their actuation mechanics, as they feature noteworthy mechanisms and assemblies [20]. Analyzing the evolution of leg link geometry over the years can yield valuable insights into this component's function which can be useful in design exoskeletons with no leg links. In previous exoskeleton designs such as those presented in [19-21] and later, we find leg links consisting of: a front support on the thigh connected by a spring to the backframe [19]; leg links connected to an actuation assembly consisting of mechanical parts such as springs, locking or release stops, etc., mounted on the front of the body, with an innovative mechanism that, despite the presence of the leg link, allows unrestricted upright walking regardless of leg stance [21]; leg links consisting of rigid material with a narrow band around the thigh for agricultural and other applications [22]; leg links consisting of rigid material with a plate pressed against the leg [23, 24]; leg links consisting of flexible materials such as textiles [25-30]. For many years, the Politecnico di Torino Department of Mechanical and Aerospace Engineering (DIMEAS) has constructed exoskeleton prototypes consisting both of rigid bodies [31-36] and textile structures [37] for rehabilitation, pressotherapy, active suits, industrial purposes, etc. Simulations and other studies have also been carried out [38]. This paper presents a new type of trunk support exoskeleton with no leg links or backframe. Pneumatic actuators are used, providing a less rigid structure and ensuring that the action of the exoskeleton on the wearer's body can be changed with ease.

2 THE NEW EXOSKELETON PROTOTYPE

The exoskeleton prototype presented here is based on DIMEAS's extensive experience with exoskeletons for industrial applications [31,32,36] and for robotic neurorehabilitation [33-35, 37].

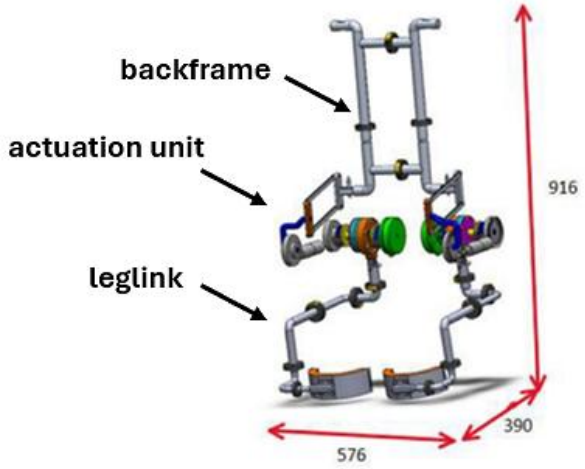

Figure 1a Earlier DIMEAS industrial trunk support exoskeleton [31,36].

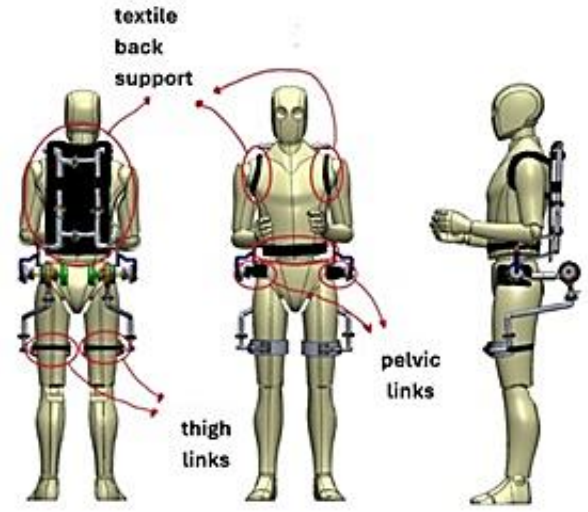

Figure 1b Details of this exoskeleton as worn [36].

Earlier industrial trunk support exoskeletons were designed with a conventional structure (Figures 1a and 1b) featuring active hip joint actuation units, a backframe carried on the wearer's back, and leg links in contact with the thigh. Optimized wearability of some of these exoskeletons is illustrated in Figures 1a and 1b [36]. In this case, the multifunctional actuation units employ electric motors. As a result of earlier studies conducted by the authors [31,32,36], these multifunction units accommodate three exoskeleton operating modes: allowing the wearer's legs to move freely during emergencies or special situations; moving the wearer's trunk in flexion or extension, providing 30% of peak muscle torque; and supporting the wearer's trunk in bending forward while stationary, when the actuation system locks the exoskeleton in the required position. To improve weights, dimensions and "legs-free" mode, the authors have designed a new geometry for an industrial trunk support exoskeleton with no leg links (Figure 2a). The new design features four pneumatic actuators at each side of the wearer's trunk (Figures 2b and 2c) that impose a rotation initially on the hip axis and then, after the physiological delay [14] between spine joint motion and hip joint motion during forward bending, on the wearer's back. Flat actuators were selected to reduce overall exoskeleton dimensions and improve wearability. Currently consisting of standard materials, these actuators can in the future be replaced with similar technopolymer actuators to further reduce weight. The backframe carried on the wearer's back was also eliminated, with an eye to having its function performed via the actuation groups themselves and a textile vest that can be stiffened if necessary by elastic bands inserted into pockets in the fabric. In this way, the top actuators move the torso C-frame slightly after the bottom actuators move the hip bar. As there are no leg links, "legs-free" mode is automatically guaranteed, with the option of immediately reducing the pressure in each cylinder, leaving the operator free to move in the event of emergencies or indisposition. To provide the delay between normal spine joint and hip joint movement [14], two devices (dubbed "delayers") were located at the end of the top rod actuators.

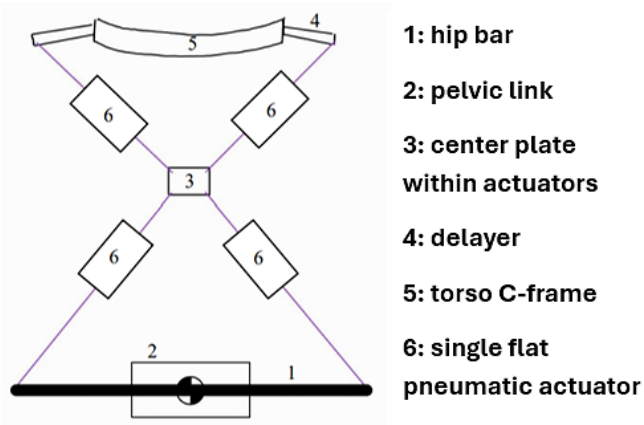

Figure 2a The new actuation unit structure.

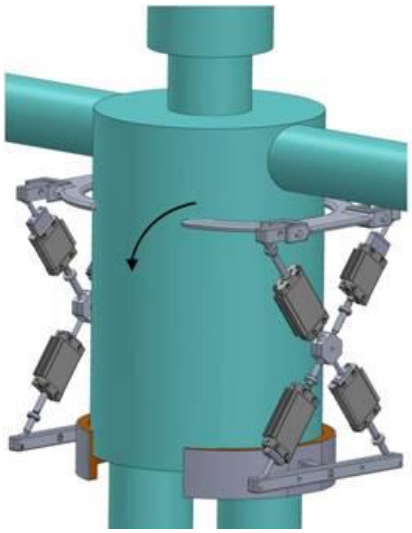

Figure 2b The new DIMEAS exoskeleton with no leg links worn by a 95%ile male.

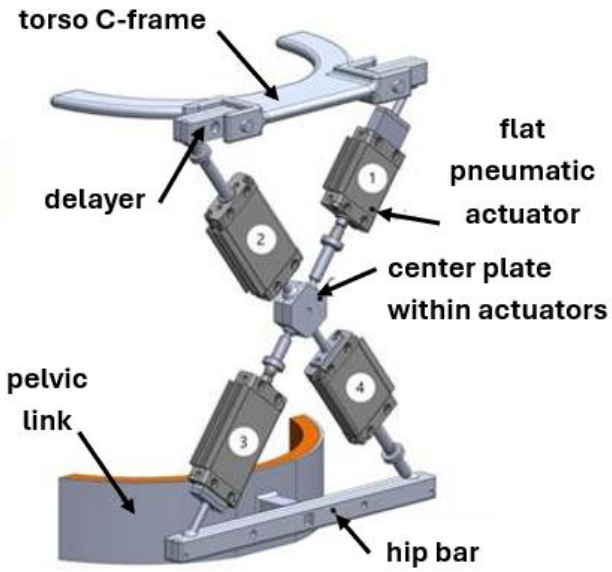

Figure 2c Details of the new DIMEAS exoskeleton with no leg links.

This actuation unit design, and the use of pneumatic actuators, also guarantee that the exoskeleton's other functions can be performed (viz., providing the required percentage of muscle torque at the hip and trunk, and fully supporting the trunk when leaning forward). Consequently, this new design also qualifies as a "multifunctional actuation unit." These units now have a pneumatic actuators, but the authors plan to design an alternative solution with electric actuators in the future. In designing exoskeletons of this type, knowledge of the human pelvis and spine is also fundamental. Accordingly, the authors reviewed key literature [12-16] and developed spreadsheets whereby they can determine the main dimensions of the human pelvis [17], especially the distance from the hip axis to the lumbosacral joint.

3 EXOSKELETON PROTOTYPE GEOMETRY AND OPERATION

As shown in Figure 3, the bottom actuators act on the hip axis by imparting a rotational motion to a bar whose length is such that the system guarantees the necessary torque-assist even at pressures below 5 bar. The top actuators act on a C-shaped component placed at a certain distance from the hip bar and called the "torso C-frame." To minimize air consumption and ensure wearer safety, the exoskeleton is designed to guarantee sufficient assistive torques with pressures below 5 bar (1 bar = 10^5 Pa). Given its structure, the actuation unit is self-balancing when the wearer is standing upright, as all four actuators are identical and supplied at the same pressure. During forward trunk flexion, the actuator axes are no longer perfectly aligned; as will be discussed below, however, this misalignment does not cause problems or place excessive forces on the wearer.

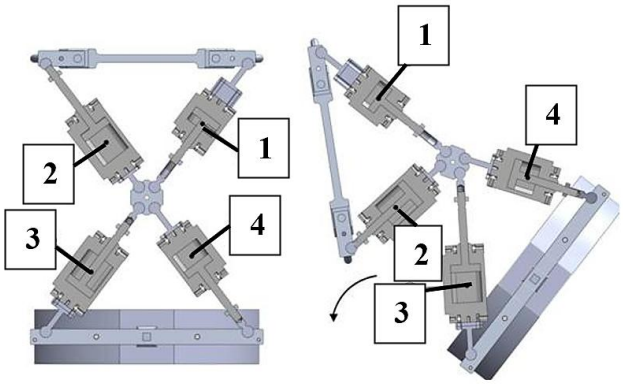

Figure 3 Details of DIMEAS exoskeleton operation.

3.1 PNEUMATIC ACTUATOR SELECTION

In selecting actuator bore and stroke, the objective was to provide the highest possible percentage of torque at the hip with pressures below 5 bar at all times. The final actuator geometry shown in Table 1 was determined on the basis of the minimum bores available in the manufacturer's catalog. Flat actuators were chosen because of the need to limit overall dimensions, improve wearability and prevent piston rotation [39]. For optimization purposes, similar commercial

Table I – Pneumatic cylinder characteristics (1 bar=10^5 Pa)

Actuator	Characteristic
Model	Festo series DZF
Bore	25 mm
Stroke	Actuator 1 = 10 mm; 2 = 40 mm; 3 = 40 mm; 4 = 25 mm
Type	Rectangular section, anti-rotation
Mass	Actuator 1 = 0.186 kg; 2 = 0.240 kg; 3 = 0.240 kg; 4 = 0.204 kg
Envisaged operating pressure	< 5 bar
Maximum operating pressure	10 bar

actuators consisting of lightweight materials such as technopolymers are now being sought.

4 WEARABILITY STUDY

Given the X-configuration of each actuation unit, it is advisable to avoid the need to make anthropometric adjustments for individual wearers which would change the distance between the hip bar and torso C-frame, and thus affect actuation unit performance and operation. Accordingly, the design of the X-configuration and the distance between the hip hinge and the C-frame was based on an in-depth anthropometric study to accommodate wearers ranging from 5th percentile women to 95th percentile men. As shown in Figures 4a and 4b (dimensions in millimeters) the current geometry will fit wearers down to 10th percentile women without modifying the arrangement of the actuation unit components. For 5th percentile women, it may be necessary to make a small geometric modification to the torso C-frame, creating a concave shape that allows the exoskeleton to fit equally well without interfering with the wearer's axillary area [40-43]

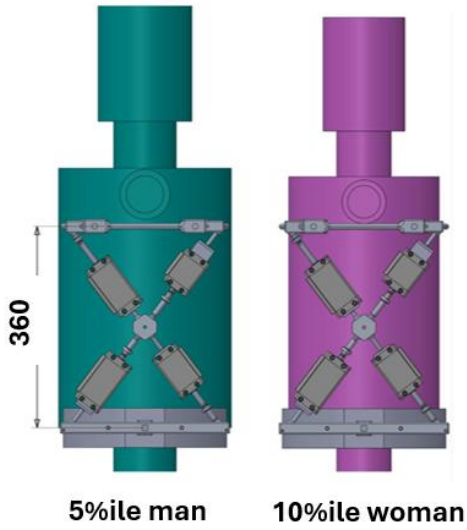

Figure 4a Distance between hip bar and torso C-frame accommodates a wide range of wearers.

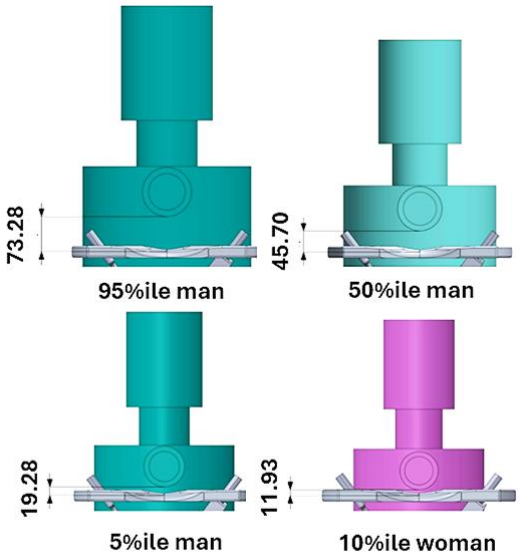

Figure 4b Distance between torso C-frame and axillary fossa in various wearers.

5 MOVEMENT STUDIES

The new exoskeleton's design was also based on experimental studies of trunk flexion. For this preliminary evaluation, a volunteer performed all movements, which were videotaped and analyzed using Tracker, a free software tool [27] (2024 version). In the future, movement studies will also be conducted with a larger number of volunteers and with pose estimation techniques using AI models (pre-trained or otherwise) developed with appropriate software as shown in Figures 5a and 5b [45,46].

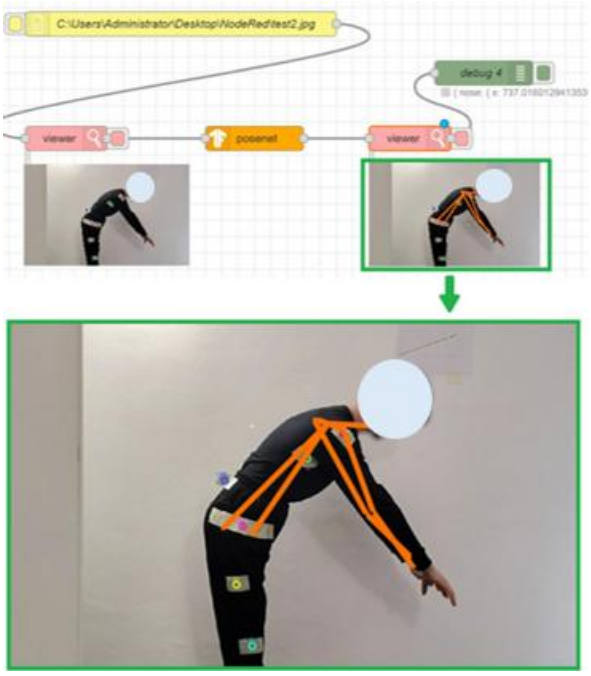

Figure 5a Pose estimation with pre-trained models in Node-RED (version 18.50, Posenet TensorFlow) [45].

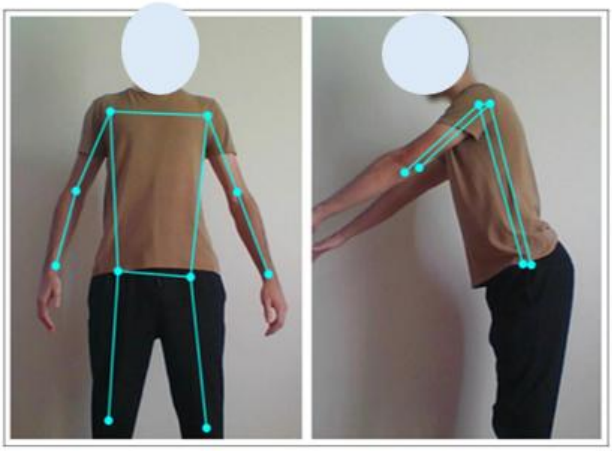

Figure 5b Pose estimation using author-trained models in Teachable Machine (version 2.0) [46].

In this exoskeleton design procedure, a single subject movement was studied because this study is focused to verify some information on this topic from the general literature but also by referring to studies and experimental tests and simulations previously conducted by the authors [.31,32,38]. The study of motion is here aimed only at the exoskeleton design and analysis the subject not wearing the exoskeleton. The authors have already begun experimental tests with other subjects and with multiple subjects (both women and men) to further their understanding of this motion in healthy individuals not wearing the exoskeleton and with the purpose only to better know this kind of movement. These studies are also now conducted by the authors using AI pose estimation models for the human body. After all these further considerations, authors will start some more verifications simulating and analyzing various kind of subjects wearing the exoskeleton.

5.1 VOLUNTEER SELECTION AND VIDEO RECORDING CONDITIONS

To expedite this initial movement study, a single volunteer was selected [12-16, 43,47,48]. Characteristic data were collected and markers were placed on the clothed volunteer so that trunk movement could be analyzed using the Tracker software. The markers were placed over the subject's clothing, since the exoskeleton will always be worn by a clothed subject. It was thus also possible to analyze clothing movements. Videos were recorded using an ordinary Android smartphone placed at a distance of 2 m from the subject. All videos were shot in the sagittal plane. A healthy volunteer's physiological trunk flexion and extension was recorded. Table II presents the volunteer's main characteristics. Studying physiological trunk motion rather than the specific motion of an individual lifting a load from the ground is essential in designing a trunk exoskeleton that respects the anatomy of the pelvis, which has two different hinges: the hip axis and the lumbosacral joint, where the spine connects to the pelvis.

It is also important to study movement dynamics to design a device that respects the delays between pelvis and spine movements [14]. A study of this type also allows for repeatability in experimental motion analysis. The exoskeleton presented here is primarily designed to support the motion of the trunk and support it when bent forward. For the moment, the case of lifting a load from the ground has not been addressed in detail.

Table II - Subject characteristics

Characteristic	Value
Gender	Male
Age	25
Profession	Mechanical engineer
Body mass	70 kg
Height	1.75 m
Right-handed/left-handed	Right-handed
Sports	Trekking
Surgical operations	None
Hip axis to lumbosacral joint	160 mm
Hip axis to axillary fossa	450 mm
Hip axis to neck attachment	550 mm
Hip axis to top of head	820 mm
Hip axis to knee axis	430 mm
Pelvis width	340 mm
Hip axis to torso C-frame	360 mm

6 EXPERIMENTAL MOVEMENT ANALYSIS

Markers were placed on the shoulder joint, at the point under the armpit where the torso C-frame will make contact, on the lumbosacral joint, on the hip axis, at the mid-point of the thigh and on the knee joint to correctly examine the entire physiological motion of the trunk in flexion and subsequent return to the upright position. Marker positions and motion angles of the trunk and of the pelvis are shown in Figures 6a and 6b. In particular authors underline that: α is the trunk angle; β is the torso C-frame forward flexion angle; θ is the pelvis angle.

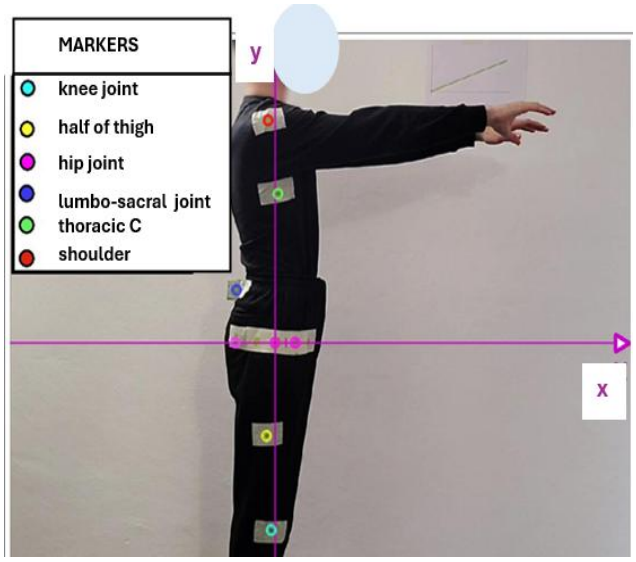

Figure 6a Markers positioned on the volunteer.

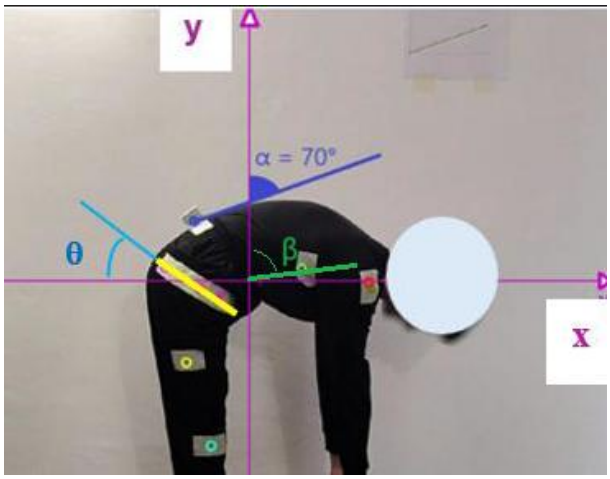

Figure 6b Motion angles used by the authors.

The experimental and theoretical curves for torso C-frame forward flexion are shown in Figure 7a. The experimental results were in complete agreement with the theoretical cycloidal law typical of this movement.
Pelvis and spine rotation angles and angular velocities are shown in Figures 7b and 7c; in particular, Figure 7c also shows motion onset and thus the physiological delay between pelvis rototranslation and trunk forward flexion [12-16].

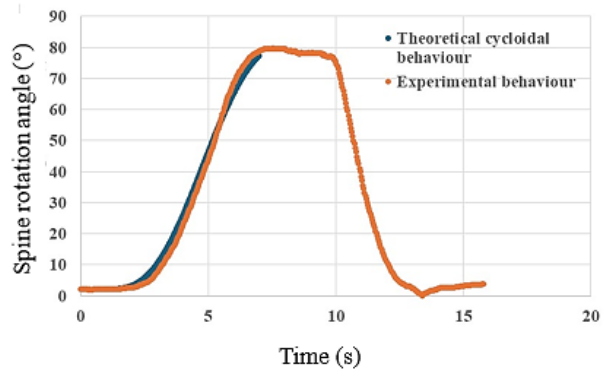

Figure 7a Experimental and theoretical curves for torso C-frame forward flexion (β angle) versus time.

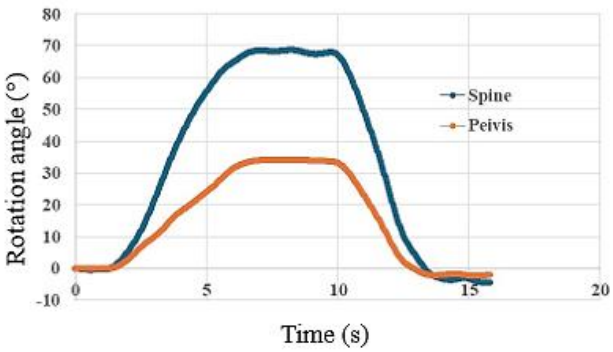

Figure 7b Pelvis (θ) and spine (α) rotation angles versus time.

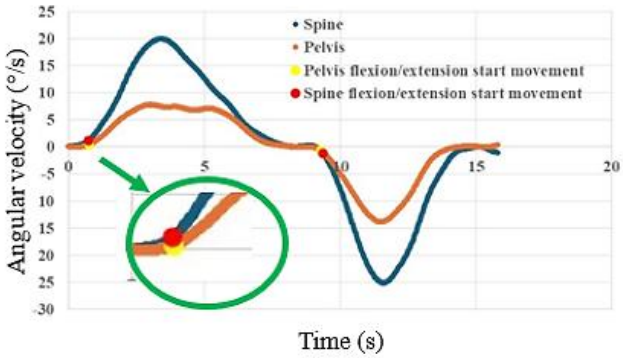

Figure 7c Pelvis and spine angular velocity versus time.

As can be seen, experimental tests and analysis are in good agreement with theory and the literature, and are consistent with normal physiological trunk motion. Figures 8a and 8b compare the current results for pelvis and spine motion during trunk forward flexion with those obtained in a preliminary experimental study carried out at DIMEAS a few years ago [32]. Current results are shown in Figure 8a, while results of the earlier tests are shown in Figure 8b. It should emphasized that the curves and displacements from the current study are consistent with those obtained in the 2019 study with different subjects and motion tracking methods [32]. During trunk flexion, the pelvis undergoes a rototranslation. In [14,15] with a trunk flexion of 63.89°, pelvic backward shift is approximately 146 mm, while under other test conditions, it is approximately 160 mm, as determined in earlier experimental tests conducted at DIMEAS (2019 with a 25 year old male subject [32]). In the current motion analysis, pelvic backward shift was approximately 130 mm. The disparities between these values are entirely acceptable in view of the differences between the subjects and testing methods.

7 EXOSKELETON OPERATION

A model of the exoskeleton worn by the volunteer was constructed in a CAD environment (SolidWorks software version 2024) (Figure 9) to check its operation during trunk flexion and determine each actuator's lever arm with respect to the hip axis and the center of the torso C-frame, thereby obtaining the torques.

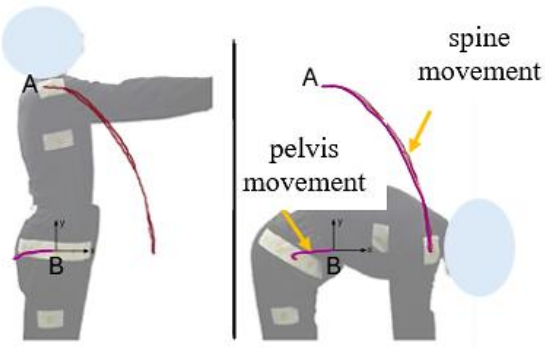

Figure 8a Pelvis and spine movements during trunk flexion determined experimentally in this study.

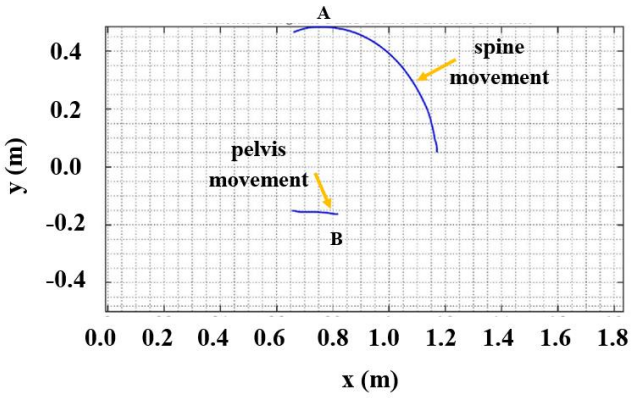

Figure 8b Pelvis and spine movements during trunk flexion determined experimentally by the authors in 2019 [32].

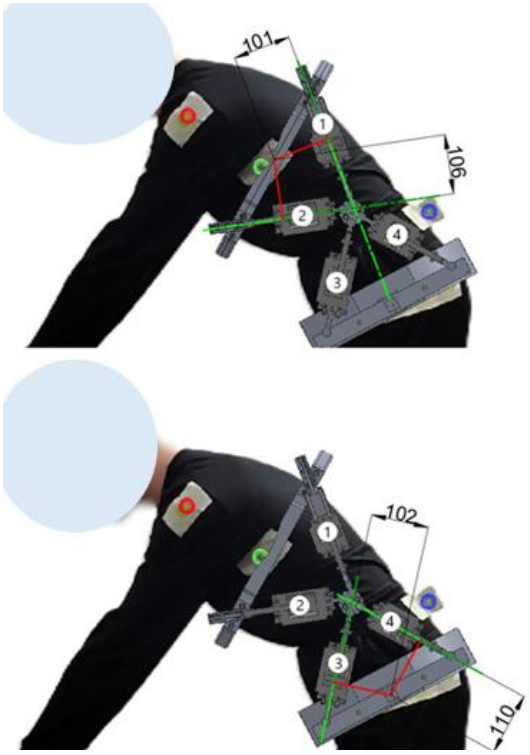

Figure 9 Cylinder lever arms relative to the hip axis and the lumbosacral joint during motion.

Obviously, exoskeleton dimensions and design have not yet been optimized. It was thus possible to evaluate lever arm variation during exoskeleton operation in trunk flexion from 0° to 70°: actuator 1 lever arm is shortened by approximately 10 mm, while that of actuator 2 remains almost constant relative to the center of the torso C-frame. Actuator 3 lever arm is shortened by approximately 10 mm, while that of actuator 4 lengthens by approximately 7 mm relative to the hip joint axis. Given this information, changes in the torque delivered by the exoskeleton during trunk flexion and extension were quantified as shown in Figures 10 a-d, where the blue bar represents the torque required with that trunk flexion angle. In particular, Figures 10a and b shows the maximum torques provided by actuators supplied at 5 bar. Practically all actuators provide much more torque than is required. Figures 10c and d show the maximum torque provided at 2 bar supply pressure. The torques thus obtained are better than those at 5 bar, as they are all lower and reduce air consumption. Supply pressure laws can thus be plotted for trunk flexion and extension (Figures 11a and 11b) to optimize the future control system. In this way, as shown in Figures 12a and 12b, all torques are optimized during movement, and are never too far above or below the maximum required muscle torque. It is important to bear in mind that the exoskeleton need only deliver a percentage of the maximum required muscle torque. This improves actuator operation and demonstrates an advantage of using pneumatic power. It can be concluded from the results reported in the bar charts (Figures 10) that having a constant power supply for the entire duration of the movement is ineffective, as it is likely to produce excessive or insufficient torques for certain trunk angles.

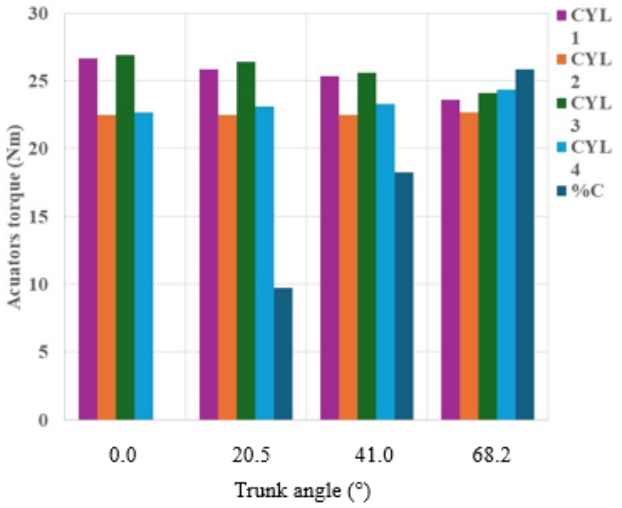

Figure 10a Actuator torque versus trunk flexion angle (supply pressure: 5 bar).

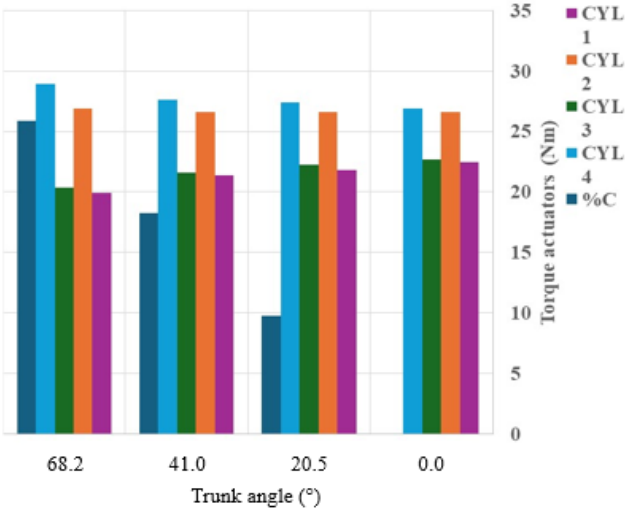

Figure 10b Actuator torque versus trunk extension angle (supply pressure: 5 bar).

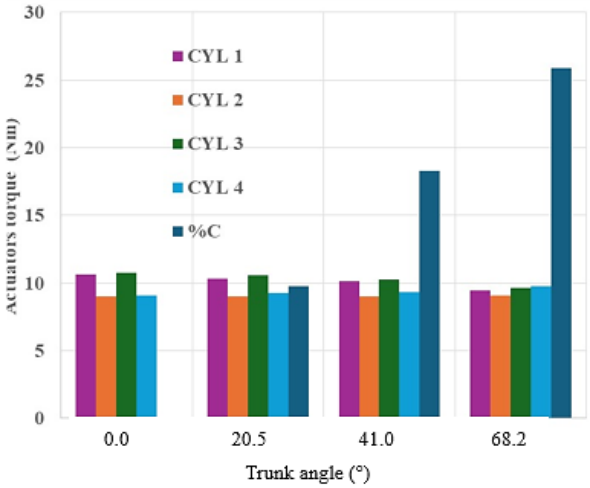

Figure 10c Actuator torque versus trunk flexion angle (supply pressure: 2 bar).

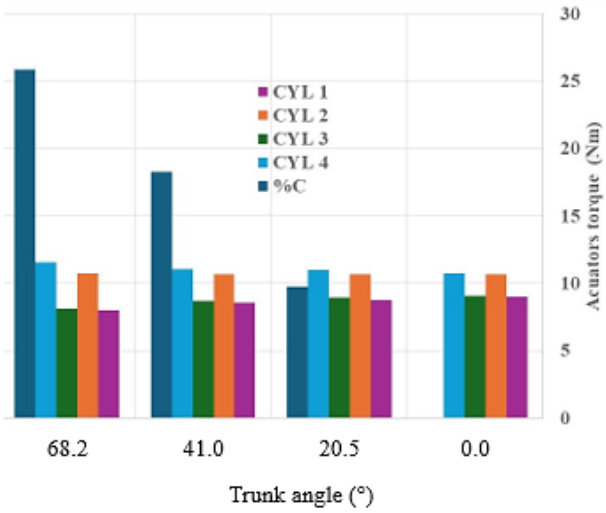

Figure 10d Actuator torque versus trunk extension angle (supply pressure: 2 bar).

A time-pressure law should thus be used to ensure that the pressure reached is sufficient to obtain the correct torque for each angular position reached over time. The supply pressure law was determined interactively in such a way as to obtain the maximum percentage of active exoskeleton support at every angle reached during flexion. It was thus possible to construct the supply pressure law that, with an appropriate control system, will optimize exoskeleton operation in all phases of trunk motion (Figures 11a and 11b). Figures 12a and 12b also show the new torque percentages that can thus be obtained. Results of this analysis are very satisfactory, and useful both for understanding actual exoskeleton operation and for designing the future control system.

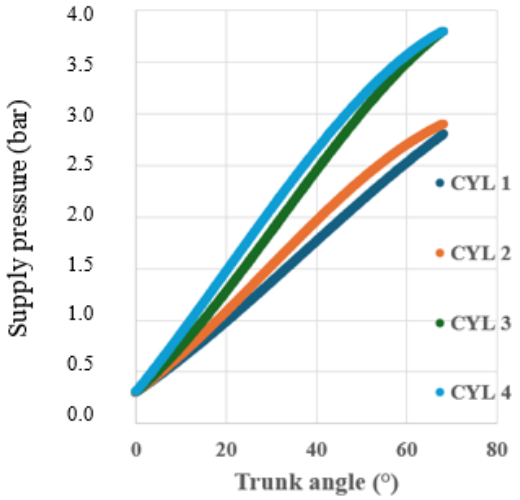

Figure 11a Optimized supply pressure versus trunk flexion angle.

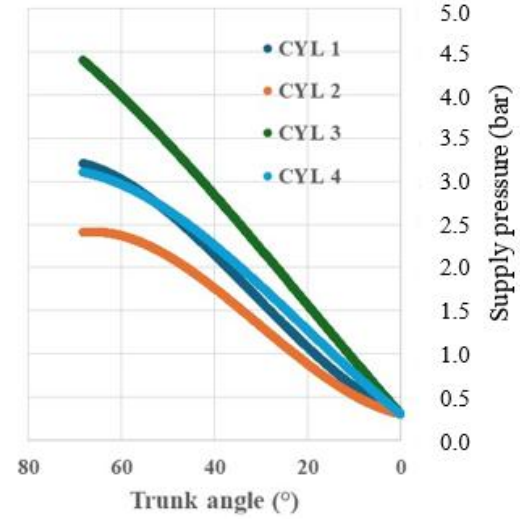

Figure 11b Optimized supply pressure versus trunk extension angle.

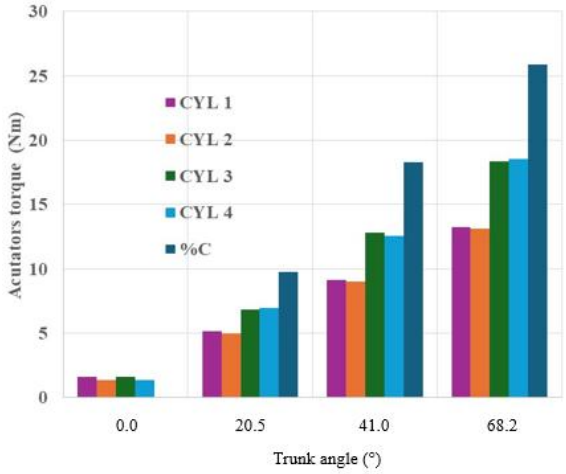

Figure 12a Actuator torque optimized via the indicated supply pressure law (trunk flexion angle).

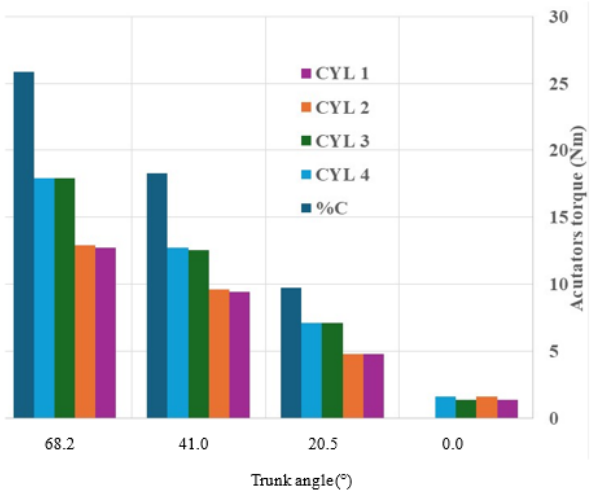

Figure 12b Actuator torque optimized via the indicated supply pressure law (trunk extension angle).

8 DELAYERS

A delay reflecting the physiological delay between spine joint motion and hip joint motion must be provided between the activation of the bottom cylinders driving the hip lever and the top cylinders driving the torso C-frame. Devices called "delayers" were thus designed that allow the top actuators to move the C-frame only after a predetermined time lapse from bottom cylinder activation [49]. With this solution, the correct delay can be provided either in parallel with the future actuator control system to ensure a high level of wearer safety, or independently (i.e., instead of the control system) to simplify the control logic. Initially, these delayers were conceived as a connecting rod hinged on one side to the C-frame and on the other to the piston of the top actuators, with an interposed damper (or spring) capable of delaying top cylinder action on the C-frame as shown in Figure 13.
Starting from this geometry, the delayers were then designed and engineered using a shock absorbing material between the actuators and C-frame. Before rigidly transmitting motion from the actuator to the C-frame, the shock absorbing material deforms viscoelastically in such a way as to create the desired delay.
A neoprene rubber with good damping properties and elasticity was selected for this purpose [49].
As shown in Figures 14a and b, the delayers are coaxial with the actuators, linked in one side to the actuator and on the other side to the C-frame. They feature a split casing consisting of two interlocking sections containing the delaying system and the mechanical transmission from the actuators to the C-frame. To study the system's dynamic behavior, the delayer is simplified into a discrete lumped parameter model, treated as a single degree-of-freedom mass-spring-damper system as shown in Figure 15a. Simulation was performed by perturbing the system using a ramp input signal, representing actuator displacement over time. By solving the differential equation, trunk displacement depends on system mass m and the neoprene rubber's damping β and elastic k values (Figure 15b).

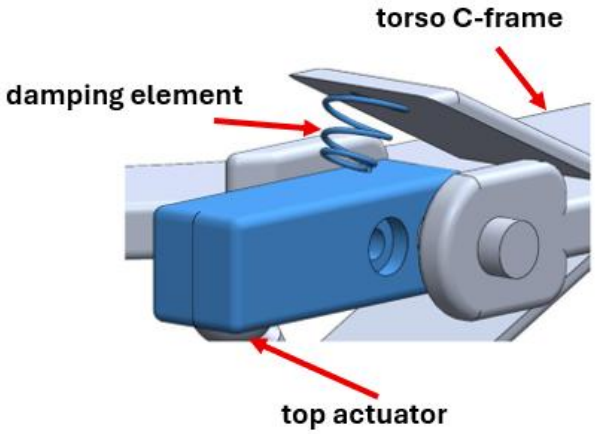

Figure 13 Preliminary delayer design.

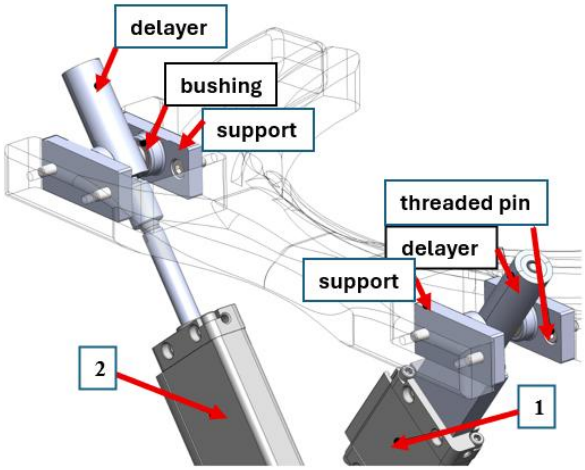

Figure 14a Main delayer assembly details.

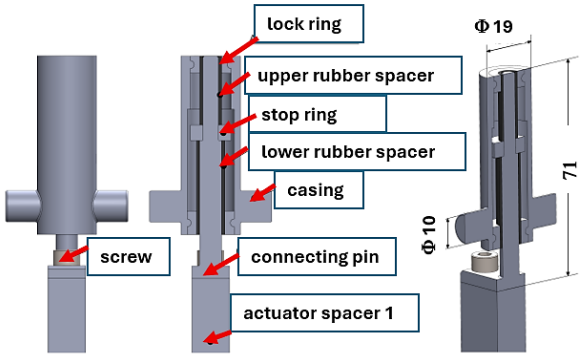

Figure 14b Delayer construction details.

Numerical simulation was performed with MATLAB Simulink software (version R2024a) and the following parameters; system mass, which depends on the mass of the human torso and the upper part of the exoskeleton, damping value, which is an intrinsic characteristic of the neoprene rubber, and the elastic propriety, which depends on the neoprene component's geometry and shape. As can be seen from the simulation results in Figure 16, the C-frame tends to follow the actuator curve, initially with an oscillatory

movement and slightly after the input signal, while at steady-state the two curves tend to coincide. The initial delay between the two signals matches the physiological delay between hip joint motion and spine joint motion, which is about 60 ms on average [14].

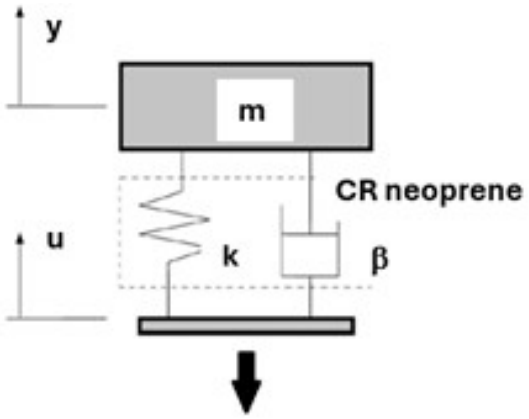

Figure 15a Delayer design model.

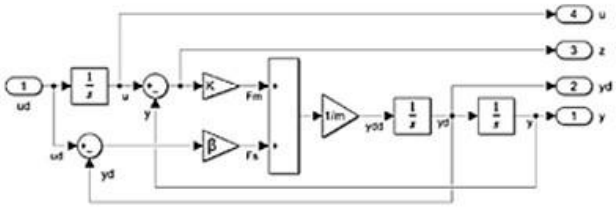

Figure 15b MATLAB Simulink model.

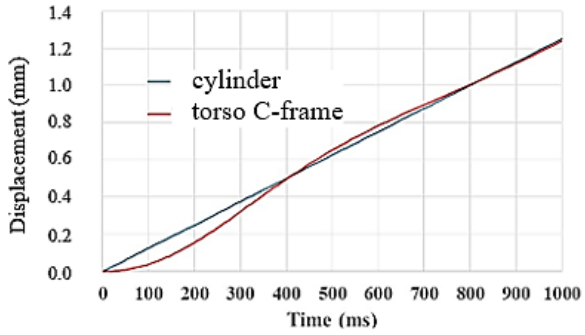

Figure 16 Selected simulation results.

Equation (1) clarifies the modelling process.

$$\ddot{y} = \frac{1}{m}[\beta(\dot{u} - \dot{y}) + k(u - y)] \rightarrow \int \rightarrow \dot{y} \rightarrow \int \rightarrow y \tag{1}$$

9 LOADS ON THE WEARER'S BODY

To better understand the interaction between the exoskeleton and the wearer, the forces exerted by the device on the wearer's body were studied under various trunk flexion angles and in the extreme and unrealistic condition in which the body acted on by the exoskeleton is considered to be inert. In reality, the body and exoskeleton are two autonomous active systems that must always move in perfect synchrony and never in opposition. Consequently, the forces exerted by the device on the body are actually lower than those calculated here. Figure 17 shows the action of each actuator (yellow) during exoskeleton operation, with their components (red) along the wearer's back and perpendicular to the wearer's body. The blue arrow indicates trunk movement. Analysis addressed only the actuator actions and their effects (difference or sum components) on the wearer's body, which was considered to be rigid and stationary.In reality, the body moves under its own muscle power in synchrony with the exoskeleton, which provides only an auxiliary torque. Again, the exoskeleton forces perceived by the wearer are actually much lower than the values obtained here.

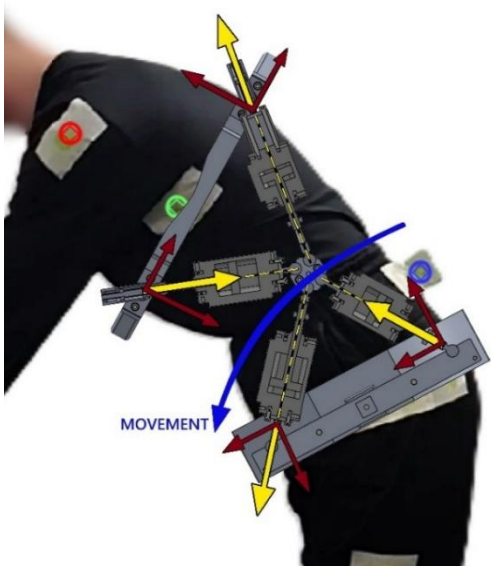

Figure 17 Details of the actuator forces along and perpendicular to the wearer's body.

Table III shows the forces exchanged between the exoskeleton and the wearer at supply pressures of 2 bar and 5 bar.

Table III - Exoskeleton forces on the wearer's body.

FORCES ON THE WEARER'S BODY		
Type	Supply pressure (bar)	Average maximum value (N)
Perpendicular pelvis (traction and compression)	5	560
	2	224
Perpendicular thoracic (traction and compression)	5	604
	2	242
Tangent to the spine (traction)	5	175
	2	70
Tangent to the abdomen (compression)	5	171
	2	68

Comparing these values with others from the literature [10,50], it was found that average forces on the wearer's body from a trunk exoskeleton vary in the literature from 120 to 150 N in traction, reducing disc compression by about 600 N during the flexion-extension cycle, with thoracic traction about 170 N and dorsal traction of 120 N. This analysis demonstrates that the prototype performance well under the conditions indicated above.

10 PRELIMINARY RISK ANALYSIS

To complete this stage of exoskeleton design, it is necessary to analyze the potential risks that may arise from the use of the exoskeleton before proceeding to address the purely technical aspects. Risk analysis for an industrial exoskeleton is carried out for several fundamental reasons, with the common goal of ensuring wearer safety and the device's effectiveness in an actual work setting [50]. These considerations are of paramount importance, as the exoskeleton is a machine that works in close contact with the wearer, meaning that safety standards must be particularly high to prevent problems that could jeopardize the wearer's health [51] [42].
Performing a risk analysis of the prototype at this stage of the design and with an eye to future design is advisable, as what the danger scenarios and their technical causes might be can be understood in advance.By identifying these critical aspects, it is possible to take action during the design phase, with the aim of arriving, at the end of prototyping and testing, at a product whose technical and functional characteristics are such as to minimize dangers for the wearer, other users and the surrounding environment [51] [42]. The method employed for the risk analysis involves identifying the prototype's operating and geometric characteristics (Table IV), defining risk scenarios for exoskeleton use (Table V) and objectively assessing the most dangerous scenarios in order to limit and/or eliminate them though changes in the device's design. The Fine-Kinney method was used to assess these scenarios.

Table IV - Main exoskeleton characteristics.

EXOSKELETON	
Type	Active, pneumatically actuated
Components	Torso C-frame Hip bars Center plates Pneumatic actuators Delayers
Total mass	9.9 kg
Dimensions [mm]	400 x 175 x 351
Adaptability	> 5 pct man > 10 pct woman
Range of movement	Forward trunk flexion 0° - 70°
Max. torque assist	18.31 Nm - top actuators 13.08 Nm - bottom actuators

Table V - Main risk analysis considerations

Hazard Classes	**Type**
Mechanical hazard	Hazards resulting from moving components, pinch points and connections between components
Thermal Hazards	Hazards resulting from component overheating, friction between parts
Noise Hazards	Hazards resulting from harmful levels of noise
Vibration Hazards	Hazards resulting from vibrations transmitted to the wearer
Ergonomic Hazards	Hazards resulting from component misalignment and non-optimal design
Max. torque assist	18.31 Nm - top actuators 13.08 Nm - bottom actuators

The Fine-Kinney method [52] is a risk assessment methodology based on mathematical calculation whereby a numerical score is assigned to a hazardous situation so that all analyzed risk scenarios can be objectively ranked.
The method uses three dimensionless parameters: likelihood, or the probability that risk scenario will occur; exposure, or the frequency with which the wearer may be exposed to the hazardous situation; and the possible consequences of the risk scenario in question. The scenario's risk score is the product of these three independent parameters [52]. As shown in Figure 18, the results show that potential hazards chiefly arise from the physical and functional interaction between the device and the wearer. Future design work will thus center on providing protective bellows around the delayers and actuators to prevent injury, crushing, or pinching of clothing or skin. Further studies will also address the materials that can be used, structural optimization to improve the components' mechanical resistance/weight ratio, and improving ergonomics by eliminating sharp edges and protrusions.

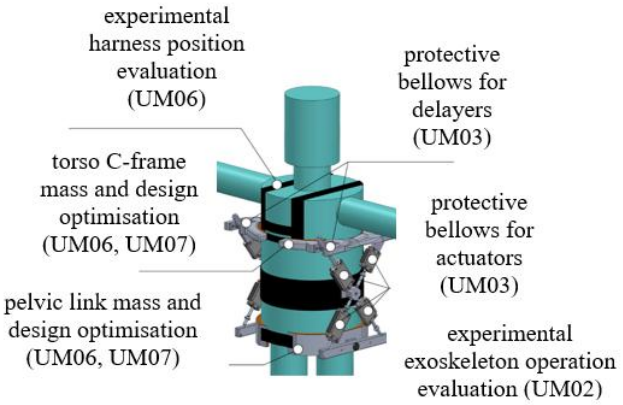

Figure 18 Summary of the risk analysis.

For a full evaluation of exoskeleton operation, moreover, a prototype must be constructed to test actual movement assistance.

11 WEARABILITY, WEIGHT AND SIZE

The analyses presented here indicate that the new trunk support exoskeleton is very versatile compared to earlier DIMEAS designs [31,32,36] or exoskeletons described in the literature [6,21], and offers good fit, low weight and compact dimensions Like earlier DIMEAS prototypes [36], it features multifunctional actuation units. To maintain the advantages of the first prototype, the exoskeleton's "X" configuration and the type and mounting direction of the actuators have been retained. Although the geometry remains unchanged, the overall height of the exoskeleton has been reduced from the first prototype's 360 mm to ensure that the device will fit a wide range of users (Figure 19a). Figures 19b and 19c illustrate the main dimensions and masses of two earlier industrial trunk exoskeleton prototypes designed at DIMEAS [31,36].

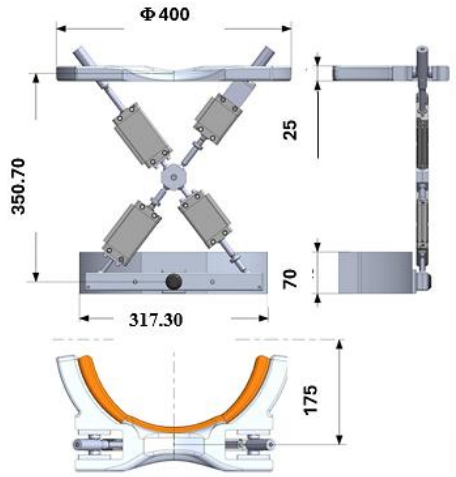

Figure 19a Main dimensions of the new exoskeleton structure (in mm).

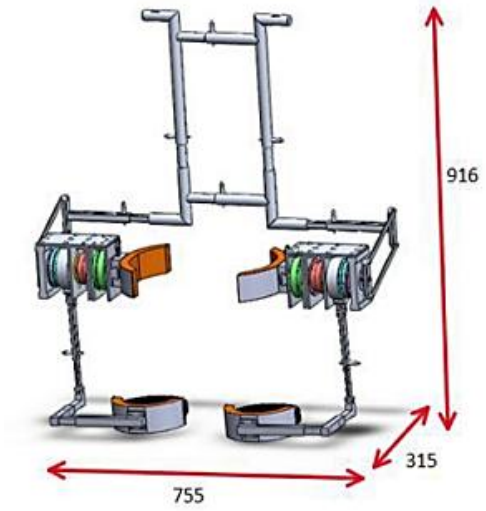

Figure 19b An earlier DIMEAS prototype with active multifunctional actuator units (dimensions in mm).

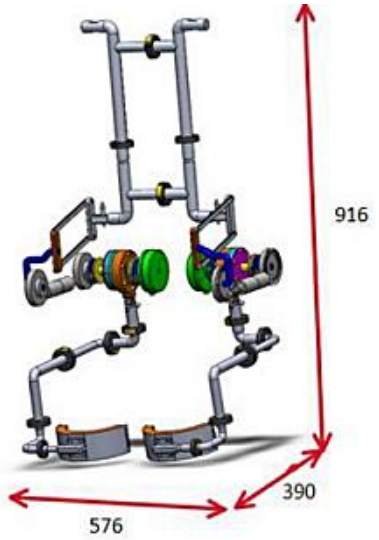

Figure 19c Optimization of the earlier DIMEAS prototype (dimensions in mm).

The advantages of the new prototype presented here are clear from a comparison with these data.

The fact that new prototype has no leg links is a particularly important advantage, as it reduces stress on the wearer, especially on the thigh, which is now free. It also permits a new geometry for the actuation units (which are always self-balancing thanks to their X-shaped arrangement and use of identical actuators), automatically ensures "legs-free" mode, and improves wearer comfort and fit. The masses of the earlier DIMEAS prototypes are respectively 5.6 kg (Figure 19b) and 5.3 kg (Figure 19c) for each actuation unit, while total mass is 9.2 kg (Figure 19b) and 8.9 kg (Figure 19c), including leg links and backframe.

Table VI shows the main materials currently constituting the prototype, which are still optimizable.

Figures 20a and 20b show the new version of the exoskeleton on a CAD model of a 95th percentile Italian male and on a volunteer.

Table VI – Main characteristics of the new prototype

Component	Material	Mass (kg)
Torso C-frame	Ergal 7075 - T6	1.90
Hip support	Ergal 7075 - T6	1.50
Hip bar	Ergal 7075 - T6	0.46
Center plate	Ergal 7075 - T6	0.06
Delayer	Delrin POM - C	0.11
Ball joint	Delrin POM - C	0.02
Spacer	Delrin POM - C	0.02
Screws	Titanium alloy	0.01
Standard pneumatic actuator	Aluminum alloy / high-alloy steel	0.87
Total mass, single actuation unit		4.95

In the future, it will be necessary to further optimize the overall weight, choosing similar technopolymer actuators and constructing the hip bar and torso C-frame using strong but lightweight polymer materials.

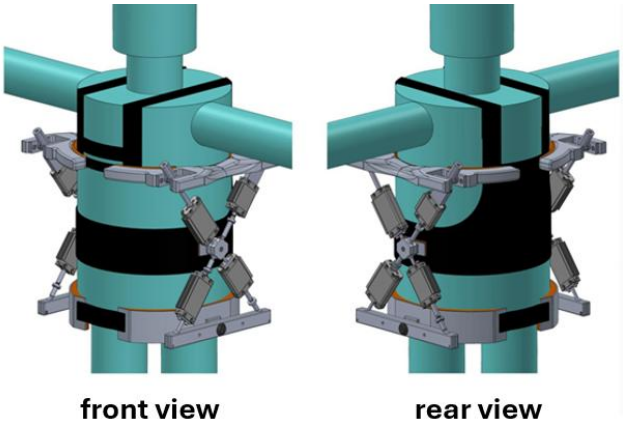

Figure 20a An example of the new exoskeleton worn by a 95%ile male.

Figure 20b CAD visualization of exoskeleton worn by a 50%ile Italian male volunteer.

11.1 MASSES AND BULK IN COMPARISON WITH THE LITERATURE

The study was then completed with a weight and size analysis of the entire exoskeleton. Comparing it with others (Table VII and Table VIII), this exoskeleton shows a good level of optimization. As shown in Table VIII, the main characteristics of the prototype presented here were compared with other exoskeletons now in production. The prototype's masses and dimensions compare very favorably, taking its great versatility into account (it assists trunk movement, supports the trunk when bent forward; can aid in lifting a load from floor level or elsewhere, etc.). In addition, the multifunctional actuation unit is designed for several exoskeleton operating modes (legs-free mode, percentage muscle torque delivery, peak muscle torque delivery, etc.). Obviously, in the future, some aspects of actuation unit and delayer design can be improved, and technopolymer actuators could be used. The exoskeleton's wearability could also be improved by reducing bulk and eliminating protruding angles. Furthermore, a textile vest will be designed to make the exoskeleton more comfortable to wear and assist its operation, for example by inserting flexible components whereby the stiffness of the vest/ exoskeleton interface can be adjusted as desired.

12 CONCLUSIONS

Based on experience gained in developing earlier exoskeletons, the study presented here led to the design of a trunk support exoskeleton with an non-conventional structure. Eliminating the leg links and backframe significantly simplifies the exoskeleton's structure without jeopardizing performance, and improves comfort and versatility while reducing weight and size as well as construction and maintenance costs.

The device was designed to fit wearers ranging from 5th percentile women to 95th percentile men without modifying the arrangement of the actuation units. This constitutes its innovative potential. Installing delayers between hip bar actuator movement and torso C-frame actuator movement reproduces the physiological hip joint and spine joint movement, greatly simplifying system geometry and avoiding the need for the additional components used in previous prototypes. The weight/dimensions of each actuation unit could be further optimized in the future, for example by using actuators of similar type but consisting of technopolymers. The analysis of the forces acting on the wearer's body, which is here assumed to be inert, provides the basis for the future development of human-machine interaction methods through instrumented experimental tests and simulation models. In any case, this preliminary analysis demonstrates the exoskeleton's effectiveness, while future analyses considering the motion of the wearer's body will show a further reduction in the forces applied to the body, a goal that will also be achieved by regulating the control pressure of each pneumatic cylinder. The study of the torque percentages during trunk flexion and the resulting pressure law will be fundamental in designing an appropriate control system. In the future, the authors plan to replace the pneumatic actuator with lightweight and space-saving electric actuation employing latest-generation electric actuators. The prototype provides multiple advantages. It has no leg links, which by definition means it is always in "leg-free" mode, and has fewer components, lower weight and costs, and is more compact. It is designed to fit a near-universal range of wearers, from 5th percentile women to 95th percentile men, while the actuation units' X-configuration makes them self-balancing when the wearer is standing upright. Minimal forces are exerted on the wearer's body during operation, which generally takes place at low pressures (2 or 3 bar) and can also be achieved with electric actuation.

Table VII – Comparison with similar devices

Ref.	Model	Producer	Main mechanical operation	Type of structure	Mass (kg)	Main points of contact with the body
[51]	Active trunk	RoboMate	DC electric actuation; motorized hip axis; leg link	Rigid	11.0	Thigh; shoulders; back; hip
[53]	ATOUN MODEL A	Panasonic	DC electric actuation; motorized hip axis; leg link	Rigid	7.4	Thigh; hip
[54]	ATOUN MODEL Y	Panasonic	DC electric actuation; motorized hip axis; leg link; small backframe	Rigid	4.4	Thigh; shoulders; back; hip
[18]	CRAY X	German Bionic	DC electric actuation; motorized hip axis; leg link; small backframe	Rigid	7.0	Thigh; shoulders; back; hip
[55]	VEX	Hyundai	DC electric actuation; motorized hip axis; leg link; small backframe	Rigid	4.5	Thigh; shoulders; back; hip
[9,10]	JAPET W	Japet	DC electric actuation	Flexible	< 2.0	Lower back
	This DIMEAS exoskeleton	DIMEAS Politecnico of Turin	Pneumatic actuation	Flexible/rigid	9.9 (improvable in the future)	Hip; crotch; chest; shoulders

Table VIII – Main characteristics of the new DIMEAS trunk support exoskeleton

Type	Pneumatically actuated active trunk support exoskeleton
Characteristics	Structure with no leg links or backframe, respecting the physiological structure of the pelvis and spine
Range of Movement	Trunk flexion from 0° to 70°
Mass	4.95 kg per side; 9.9 kg overall
Dimensions	400 x 175 x 351 mm
Wearability	Fits wearers from 5%ile women to 95%ile men
Harness	Vest consisting of polymer fabric and foam with shoulder, chest, lower back and crotch straps
Main materials	Ergal 7075 – T6 and Delrin POM - C
Maximum hip torque assist	18.31 Nm (70% maximum muscle torque)
Maximum force perpendicular to the body	Pelvic area: 5 bar 560 N; 2 bar 224 N Torso area: 5 bar 604 N; 2 bar 242 N
Maximum traction/compression force on wearer	Along spine: 5 bar 175 N; 2 bar 70 N Abdomen: 5 bar 171 N; 2 bar 68 N
Future design changes to avoid danger scenarios	Design and mass optimization; design of protective casings for moving parts; possible experimental evaluation of exoskeleton operation and fit; further study of the textile vest and exoskeleton/wearer

Lastly, the exoskeleton is multifunctional, as it provides trunk support, assists in lifting loads, reduces effort when holding demanding postures, etc. The authors are already conducting experimental studies on pose estimation using AI tools on various healthy subjects, as well as optimizing the exoskeleton itself. Specifically, its design and fit have been improved, and a possible solution using small, latest-generation electric actuators is being evaluated. This will determine the best final geometry to minimize the prototype's weight and size. In the future a strategy useful to have a potential indicator of the mechanical efficiency of the device will be set by the authors and all these indications with some more optimizations and studies on this human body movement will be taken in consideration before the device final construction. In particular the effectiveness of a torso exoskeleton can be assessed in various ways, such as: muscle activity analysis (EMG) to measure lumbar support, postural biomechanics (flexion angles), subjective perception of comfort, and ergonomic risk indices (such as NIOSH or EAWS). Specifically, a kinematic and postural analysis, including simulations, could be performed on a healthy subject wearing the exoskeleton. This allows for range of motion (ROM) assessments, as a good device reduces lumbar torque without interfering with natural gait, flexion, or the execution of daily maneuvers in the workplace. A subjective assessment of comfort, fit, size, and weight of the device itself, as well as any constraints during specific movements, can also be performed, also using ergonomic risk indices

ACKNOWLEDGEMENTS
The authors would like to thank I. Pappada', C. Vigenti, A.C.A. Borello, L. Carchia, P.D Cairella, M. Autino, F. Gorraz and S. Biglia for their help during this study.

REFERENCES

[1] Fellag R., Guiatni M., Hamerlain M. and Achour N., Exoskeleton robust control using adaptive finite time homogeneous higher order sliding modes. *International Journal of Mechanics and Control*, Vol. 22, No. 2, pp. 95-106, 2021.

[2] Polygerinos P., Wang Z., Overvelde J.T.B., Galloway K.C., Wood R.J., Bertoldi K. and Walsh C.J., Modeling of soft fiber-reinforced bending actuators. *IEEE Transactions on Robotics*, Vol. 31, No. 3, pp. 778-789, 2015.

[3] Sanchez-Lopez C., Planning handwriting for a 2-dof planar robot arm. *International Journal of Mechanics and Control*, Vol. 25, No. 1, pp. 115-121, 2024.

[4] Petuya V., Macho E., Altuzarra O., Pinto C. and Hernández A., Educational software tools for the kinematic analysis of mechanisms. *Computer Applications in Engineering Education*, Vol. 22, No. 1, pp. 72-86, 2011.

[5] Abane, A., Guiatni, M., Ababou, N., Amine Alouane M. and Bouzid, Y., Mechatronics design and control of a transformed upper limb rehabilitation exoskeleton. *International Journal of Mechanics and Control*, Vol. 21, No. 1, pp. 75-90, 2020.

[6] Marcheschi S., Salsedo F., Fontana M. and Bergamasco M., Body extender: whole body exoskeleton for human power augmentation. *2011 IEEE International Conference on Robotics and Automation*, Shanghai China 9-13 May 2011, doi: 10.1109/ICRA.2011.598132, pp. 611-616, 2011.

[7] Toxiri S., Matthias B., Näf M.B., Lazzaroni M., Fernández J., Sposito M., Poliero T., Monica L., Anastasi S., Caldwell D.G. and Ortiz J., Back-Support Exoskeletons for Occupational Use: An Overview of Technological Advances and Trends. *IISE Transactions on Occupational Ergonomics and Human Factors*, Vol. 7, No. 3-4: Occupational Exoskeletons, pp. 237-249, 2019.

[8] Petrone G., D'Alessandro V. and Sanchez-Lopez C., Planning handwriting for a 2-dof planar robot arm. *International Journal of Mechanics and Control*, Vol. 25, No. 1, pp. 115-121, 2024.

[9] Moulart M., Olivier N., Giovanelli Y. and Marin F., Subjective assessment of a lumbar exoskeleton's impact on lower back pain in a real work situation. *Heliyon*, Vol. 8, e11420, 2022.

[10] Reimeir B., Calisti M., Mittermeier R., Ralfs L. and Weidner R., Effects of back-support exoskeletons with different functional mechanisms on trunk muscle activity and kinematics. *Wearable Technologies*, Vol. 4, e12-1-e12-18, 2023

[11] Yang X., Huang TH., Hu S.Y.H., Zhang S., Zhou X., Carriero A., Yue G. and Su H., Spine-Inspired Continuum Soft Exoskeleton for Stoop Lifting Assistance. In: *IEEE Robotics and Automation Letters*, Vol. 4, No. 4, pp. 4547-4554, 2019.

[12] Legaye J., The Sagittal Pelvic Thickness: A Determining Parameter for the Regulation of the Sagittal Spinopelvic Balance. *ISRN Anatomy*, Vol. 2013, pp. 1-9, 2013.

[13] Tafazzol A., Arjmand N., Shirazi-Adl A. and Parnianpour M., Lumbopelvic rhythm during forward and backward sagittal trunk rotations: Combined in vivo measurement with inertial tracking device and biomechanical modeling. *Clin Biomech (Bristol) Elsevier*, Vol. 29, No. 1, pp. 1-13, 2014.

[14] Thomas, James S. and Gibson, Gary E., Coordination and timing of spine and hip joints during full body reaching tasks. *Hum Mov Sci Elsevier*, Vol. 26, No. 1, pp.124-140, 2007.

[15] Shin S. and Yoo W., The effect of sagittal hip angle on lumbar and hip coordination and pelvic posterior shift during forward bending. *European Spine Journal*, Vol. 29, No. 7, pp. 438–445, 2020.

[16] Vazirian M., Van Dillen L. and Bazrgari B., Lumbopelvic rhythm during trunk motion in the sagittal plane: A review of the kinematic measurement methods and characterization approaches. *Physical Therapy and Rehabilitation*, Vol. 3, No. 1, pp. 1-5, 2016.

[17] Eula G., Gorraz F., Mazza L. and Raparelli T., An engineering study of the human pelvis using models and data from the literature. *International Journal of Mechanics and Control*, Vol. 26, pp. 43-54.
[18] https://www.germanbionic.com/.
[19] Kelly R.E., *Back Brace*, Patent No. 1,202,851, United States Patent Office, 1916.
[20] Ferguson D.L. and Batton L.M.N., *Torso assist Orthotic device*, US Patent No. 8,568,344 B2, 2013.
[21] Babcock M.A., *Personal upper body support device for lower back muscle assist*, US Patent No. 7,744,552 B1, 2010.
[22] https://www.ulsrobotics.com/en/h-col-130.html.
[23] https://www.hyundainews.com/en-us/releases/230.
[24] https://www.laevo-exoskeletons.com/en/flex,
[25] https://germanbionic.com/en/press-and-download-area/.
[26] https://www.auxivo.com/omnisuit.
[27] https:// www.wirobotics.com/ product/ productDetail/ avMTG3bD.
[28] https://as.virgo.co.jp/pro3-en.html.
[29] https://www.skelex.com/products.
[30] Toxiri S., *An active back-support exoskeleton to reduce spinal loads: actuation and control strategies*. Dissertation, IIT and University of Genova (Italy), Department of Advanced Robotics, January 2018, pp. 1-100, 2018.
[31] Raparelli T., Eula G., Mazza L., Ivanov A., Pietrafesa F., Mala R. and Pontin M., A preliminary prototype of an industrial exoskeleton for the operator's trunk support. *International Journal of Mechanics and Control*, Vol. 23, No. 2, pp. 37-52, 2022.
[32] Raparelli T., Eula G., Mazza L., Ivanov A., Pietrafesa F., Mala R. and Pontin M., The design of an innovative active exoskeleton prototype for industrial application with a pneumatic actuation. *International Journal of Mechanics and Control*, Vol. 23, No. 2, pp. 61-72, 2022.
[33] Belforte G. and Eula G., Design of an active-passive device for human ankle movement during functional magnetic resonance imaging analysis. *Proc. IMechE, Part H: Journal of Engineering in Medicine*, Vol. 226, No. 1, pp. 21-32, 2011.
[34] Belforte G., Eula G., Appendino S., Geminiani G.C., Zettin M. and Sacco K., Active orthosis for the motion neurological rehabilitation lower limbs, system comprising such Orthosis and process for operating such system. *EP 2 825 146 B1*, Patent of POLITECNICO DI TORINO, 2012.
[35] Belforte G., Raparelli T., Eula G., Sirolli S., Appendino S., Geminiani G.C., Geda E., Zettin M., Virgilio R. and Sacco K., Study and realisation of a preliminary control system for the active exoskeleton called P.I.G.R.O., suitable for unloaded robotic neurorehabilitation treatments, *International Journal of Mechanics and Control*, Vol. 22, No. 1, pp. 125-142, 2021.
[36] Raparelli T., Mazza L. and Eula G., Study concerning design and optimization of a multifunction actuation group for an industrial exoskeleton. *IFIT 2024 September 2024* Politecnico di Torino, Torino Italy, IFToMM Italy 2024, Volume II, MMS 164, Chapter 1, pp. 3-10, 2024.
[37] Belforte G., Eula G., Ivanov A., Raparelli T. and Sirolli S., Presentation of textile pneumatic muscle prototypes applied in an upper limb active suit experimental model. *The Journal of The Textile Institute*, Vol. 109, No. 6, pp. 757-766, 2018.
[38] Eula G., Modeling a subject wearing an industrial trunk support exoskeleton. *International Journal of Mechanics and Control*, Vol. 26, No. 1, pp. 103-118, 2025.
[39] Flat cylinders EZH/DZF/DZH - data sheet. Festo S.p.A
[40] UNI EN ISO 7250-1: Basic human body measurements for technological design - Part 1: Body measurement definitions and landmarks. Geneva, CH: International Organization for Standardization ISO, 2017
[41] UNI CEN ISO/TR 7250-2: Basic human body measurements for technological design - Part 2: Statistical summaries of body measurements from national population. Geneva, CH: International Organization for Standardization ISO, 2024
[42] UNI/TR 11959:2024-2: Sicurezza e salute nell'uso degli esoscheletri occupazionali orientati ad agevolare le attività lavorative. Milano, IT: Ente Nazionale Italiano di Unificazione, UNI, 2024.
[43] Herman I.P., *Physics of the Human Body*. 2nd Edition, Springer Verlag, pp. 1-980, 2016.
[44] https://opensourcephysics.github.io/tracker-website/ "Tracker Video Analysis and Modeling Tool."
[45] Node-Red, OpenJS Foundation & Contributors. url: https://nodered.org
[46] Teachable Machine, Google. url: https://teachablemachine.withgoogle.com/
[47] Winter D.A., *Biomechanics and motor control of human movement*, 4th edition. Waterloo, CA: Wiley, pp. 1-370, 2009.
[48] Davidovits P., *Physics in Biology and Medicine*. Complementary Science Series Academic Press Elsevier, 3rd Edition, pp. 1-328, 2008.
[49] Chung D.D.L., Review: Material for vibration damping. *J. of Materials Science*, Vol. 36, pp. 5733-5737, 2001.
[50] Qi K., Yin Z., Li C., Zhang J. and Son J., Effects of a lumbar exoskeleton that provides two traction forces on spinal loading and muscles. *Frontiers in Bioengineering and Biotechnology*, Vol. 13, pp. 1-12, 2025.
[51] Van der Vorm J., de Looze M., Hadziselimovic M. and Heiligensetzer. P., *Risk assessment of Robo-Mate, an exoskeleton for workers*. White Paper www.robo-mate.eu, RoboMate, May 2016, pp. 2-19, 2016.
[52] Kinney G.F, and Wiruth A.D., *Practical Risk Analysis for Safety Management*. Naval Weapons Center California, pp. 1-21, 1976.
[53] https://news.panasonic.com/global/topics/5202.
[54] https://news.panasonic.com/global/topics/5214.
[55] https://robotics.hyundai.com/en/unveiled-robots/wearable/vex.do.